Textures and Microstructures, Vol. 32, pp. 119–136
Reprints available directly from the publisher
Photocopying permitted by license only

INFLUENCE OF THE SECONDARY RECRYSTALLIZATION TEMPERATURE ON THE SHARPNESS OF GOSS SECONDARY RECRYSTALLIZATION TEXTURE

JONG SOO WOO[a], CHAN-HEE HAN[a], BYUNG-DEUG HONG[a] and JIROU HARASE[b,*]

[a]*Technical Research Laboratories, Pohang Iron & Steel Co. Ltd., Pohang, Kyungbuk, Korea;* [b]*Graduate school of Iron and Steel Technology, Pohang University of Science & Technology, Pohang, Kyungbuk, Korea*

(Received in final form 28 September 1997)

Primary recrystallized Fe–3%Si specimens containing Al and nitrided were annealed intermittently with the heating rate of 15°C/h in 100% N_2 atmosphere. The magnetic induction B8 was measured after each annealing. The onset of secondary recrystallization was detected by the rapid rise of B8. The maximum B8 obtained was about 1.94 T when the onset temperature of the secondary recrystallization was around 1075°C regardless of the initial grain size or nitrogen content.

The same primary specimens were coated with MgO and annealed with the same heating rate in 5% H_2–N_2. The maximum B8 obtained was nearly same as with the above annealing condition, however, the initial grain size and nitrogen content was quite contrary in this annealing. The difference in the optimum grain size and nitrogen content for obtaining the highest B8 between both annealings was explained on the assumption that $\Sigma 9$ boundaries become most mobile at 1075°C regardless of the annealing methods. Based on this finding, the possibility of producing grain oriented silicon steel without hot band annealing and nitriding treatment was shown.

Keywords: Primary recrystallization; Secondary recrystallization; AlN; Inhibitor; Magnetic induction; Coincidence boundary

* Corresponding author.

1. INTRODUCTION

The production of grain oriented silicon steel has been initiated by Armco steel utilizing the invention by N.P. Goss (1934). This method utilizes MnS as an inhibitor, and the two stage cold rolling method is employed in this method.

In 1968, Nippon steel succeeded in the production of a new grain oriented silicon steel with high permeability called HI-B (Taguchi and Sakakura, 1964). This method utilizes AlN and MnS as inhibitors and a one stage cold rolling method. In 1973, Kawasaki steel also succeeded in the production of a new grain oriented silicon steel with high permeability called RG-H (Goto *et al.*, 1975). The grain oriented silicon steels in the world now are mainly produced by the above three methods. High temperature slab reheating over 1300°C is required to secure fine precipitates as inhibitors in these methods. High slab reheating temperature, however, causes various troubles in the production of grain oriented silicon steel. The development of the low slab reheating technology has been one of the largest targets in the research and development in this field.

In 1995 Nippon steel announced in detail the metallurgical principles of producing HI-B by low slab reheating temperature as 1150°C (Nakayama *et al.*, 1996; Takahashi and Harase, 1996; Takahashi *et al.*, 1996; Ushigami *et al.*, 1996a,b,c,d; Yoshitomi *et al.*, 1996) through nitriding after decarburization annealing and forming AlN as an inhibitor in the stage of secondary recrystallization annealing (herein after referred to as SL).

Many similarities in the technology and metallurgy are found in HI-B and SL by comparing the reports about HI-B (e.g. Harase *et al.*, 1987) and SL. The main chemical composition and the basic processing condition after hot rolling are almost the same except for the nitriding treatment after decarburization annealing in the case of SL. Namely the requirements of the high temperature hot band annealing followed by rapid cooling and the heavy cold rolling as 87% reduction before decarburization annealing. Therefore the primary recrystallization texture is quite similar in HI-B and SL and the secondary recrystallization behavior is also quite similar. It is well known that the texture, structure and the inhibitor intensity determines the sharpness of Goss secondary recrystallization texture. Further innovation of the

technology of producing grain oriented silicon steel will be expected through the investigation of the mechanism of secondary recrystallization utilizing SL material as in this case is rather easy to control these parameters.

2. SHG METHOD

In the investigation of grain growth processes it is necessary to know the grain boundary character between grains directly in contact with each other at the onset of grain growth but also between grains not directly in contact as during grain growth new contacts are made. In this connection, an analytical technique called SH method (Simulation by Hypothetical nucleus) has been developed (Harase *et al.*, 1985). In the SH method, measurements are made of several hundreds of grains in the matrix utilizing ECP or EBSP. The orientation relationships are then calculated between these grains and a specified nucleus orientation. The specified orientation can be arbitrary but is usually chosen to be one of those observed to exist in the final texture after grain growth. An analysis is then made of the relationship between the frequency distribution of coincidence orientations so found and the texture evolved by grain growth.

The SHG method has also been developed to analyze texture evolution by grain growth (Shimizu *et al.*, 1990). In the SHG method, three dimensional orientation distribution obtained by the vector method (Ruer *et al.*, 1979) from the pole figures measured by X-ray are used as an alternative to using grain orientation measurements by ECP or EBSP. In the vector method, the unit triangle T_1 representing plane normal is divided into 36 "boxes" of equal angular areas and numbered 1–36. A representative orientation (HKL) is assigned to each "box". Rotations about this orientation are divided into 72 intervals at steps of 5°. Another unit triangle T_2 of the mirror symmetry with T_1 is required to represent all orientation space, any orientation can be classified by either of 5184 orientations.

As most of the orientations are represented by 1296 orientations due to the symmetrical nature of the existing textures, these 1296 orientations are used in the SHG method to represent orientation space. Coincidence orientations from Σ1 to Σ33c with respect to each of the

1296 orientations are then calculated. In the calculation of coincidence orientation, Brandon's criterion (1966) is used. The intensity of the Σi coincidence orientation in relation to a nucleus orientation N is expressed as $I_c\Sigma$i. The intensity of the nucleus orientation N is expressed as I_N. $I_c\Sigma$i is calculated for the given texture before grain growth. The probability of selective growth of a nucleus grain can be considered to be associated with the number of the nucleus grains in the matrix as well as the number of the coincidence-oriented grains on the assumption that coincidence boundaries (except Σ1 and Σ3) are more mobile than random boundaries.

Therefore, $P_{CN}\Sigma i = I_c\Sigma i \times I_N$, the product of the $I_c\Sigma$i and the intensity I_N of the nucleus orientation (N), is calculated. Then the relationship between the texture evolved by grain growth and $I_c\Sigma$i or $P_{CN}\Sigma$i are examined to clarify the role of the coincidence boundaries on texture evolution by grain growth. In the one stage cold rolling method, $\{110\}\langle001\rangle$ has the highest $I_c\Sigma9$ values among any other orientations in the matrix before grain growth and the $I_c\Sigma9$ value of $\{110\}\langle001\rangle$ is the highest among any other $I_c\Sigma$i in the matrix before grain growth. The frequency of secondary recrystallized grains is proportional to the $I_c\Sigma9$ values and no secondary recrystallized grains exist which have lower $I_c\Sigma9$ value than the critical value in the matrix before grain growth and no distinct relationship is existing between the frequency of secondary recrystallized grains and I_N. The evolution of the sharp $\{110\}\langle001\rangle$ secondary recrystallization texture in the one stage cold rolling method is considered to be due to the sharp distribution of $I_c\Sigma9$ values around exact $\{110\}\langle001\rangle$ orientation and the specific migration characteristics of $\Sigma9$ boundary under inhibitor.

In the case of the two stage cold rolling method, however, the $I_c\Sigma9$ value of $\{110\}\langle001\rangle$ orientation is lower than the critical value required for the onset of secondary recrystallization in the one stage cold rolling method (about 60% of the maximum value of the one stage method) and the distribution of $I_c\Sigma9$ values is almost flat along $\{110\}\langle UVW\rangle$ orientation. However, the $P_{CN}\Sigma9$ is the highest at $\{110\}\langle001\rangle$ orientation. The frequency of secondary recrystallized grains is proportional to the intensity of $P_{CN}\Sigma9$ and I_N and no secondary recrystallized grains exist when the intensity of $P_{CN}\Sigma9$ is lower than the critical value (Harase and Shimizu, 1990). The sharpness of secondary recrystallized grains is mainly determined by the sharpness of nucleus orientation itself. It is therefore concluded that the sharp Goss secondary recrystallization

texture is evolved if the migration characteristics of Σ9 boundaries is well controlled in the one stage cold rolling method. It is necessary to control the nucleus orientation distribution to evolve sharp Goss secondary recrystallization texture in the case of two stage cold rolling method. It is not known so far how to control the intensity distribution of nucleus orientation.

3. INFLUENCE OF THE SECONDARY RECRYSTALLIZATION TEMPERATURE ON THE SHARPNESS OF SECONDARY RECRYSTALLIZATION TEXTURE

3.1. Introduction

It has been reported quite recently that both Σ9 boundaries and random boundaries become very mobile above certain critical temperature (herein after referred to as T_{mj} as the mobility jumps above this temperature) utilizing relatively pure Fe–3%Si bicrystal (Tsurekawa *et al.*, 1996). T_{mj} is lower in the case of Σ9 boundaries compared to that of random boundaries and T_{mj} shifts to higher temperature with decreasing driving force (grain size). In the bicrystal experiment mentioned above, no inhibitor is deliberately added. When the inhibitor is added, we assume that the T_{mj} of Σ9 will shift to higher temperature due to the pining effect of the inhibitor and that only very little boundary migration occurs both in Σ9 boundaries as well as random boundaries until the temperature reaches T_{mj} of the Σ9 boundaries. Above T_{mj} of Σ9 boundaries and under T_{mj} of random boundaries, Σ9 boundaries selectively become mobile and the relative mobility of Σ9 boundaries is larger compared with the situation without inhibitor. It is then considered that the Goss orientation, which has the highest probability of coming in contact with Σ9 boundaries, will selectively start to grow and get what is called a size advantage, namely the onset of secondary recrystallization (herein after the onset temperature of secondary recrystallization is referred as T_{cr}), when the Σ9 boundaries reaches T_{mj} in the heating stage of secondary recrystallization annealing.

As the T_{cr} is so associated with the T_{mj}, T_{cr} will become higher with decreasing driving force (increasing in grain size). This fundamental experiment suggests that grain size and secondary recrystallization temperature are closely associated with each other. In this connection

the relationship between T_{cr} and the sharpness of Goss secondary recrystallization texture was investigated.

3.2. Experimental Procedure

Thick specimens (2.3 mm) hot rolled with 1100°C slab reheating temparature (C: 0.015, Si: 3.21, Mn: 0.07, P: 0.10, S: 0.007, Cu: 0.17 & 0.33, Al: 0.03, Sn: 0.05, N: 0.008, Bi: 0.10 mass% the rest Fe and impurities) were subjected to heat treatment of 900°C × 120 s → 0°CW.Q. They were then cold rolled to 0.29 mm. Aging treatment of 250°C × 20 min was given at the thicknesses of 1.6 mm, 1.2 mm, 0.8 mm, 0.6 mm, 0.4 mm respectively during cold rolling process.

They were then decarburized in a wet atmosphere (75%H_2–N_2, D.P.: 69°C) for 40 s in the temperature range between 840°C and 920°C. The grain size after decarburization annealing was in the range between 14.8 and 22.2 μm. Then they were nitrided at 750°C for 120 s in NH_3–H_2 atmosphere. The nitrogen contents after nitriding were in the range between 183 and 793 ppm. They were subjected to Model anneal and Box anneal. In the Model anneal, the specimen was heated up to 1055°C with the heating rate of 10°C/s in dry (D.P. < −60°C) N_2 atmosphere without MgO coating on the surface of the specimen and then heated up to 1065°C with the heating rate of 15°C/h and cooled down to room temperature and B8 was measured. Then the specimen was again heated up to 1065°C with the same heating rate of 10°C/s and heated up to 1075°C with the heating rate of 15°C/h and cooled down to room temperature and B8 was again measured. In this way heating and measurement was carried out until the temperature reached 1175°C. In the case of Box anneal, specimens coated with MgO were heated in 5%H_2–N_2 atmosphere with the same heating rate of 15°C/h up to 1200°C. Then they were kept for 20 h at 1200°C in 100%H_2 atmosphere and cooled down to room temperature. After stress relief annealing, magnetic induction B8 was measured.

No specimens were extracted from the furnace to check the onset temperature of secondary recrystallization.

3.3. Results and Discussion

3.3.1. Model Anneal

Figures 1 and 2 show the relationship between magnetic induction B8 and secondary recrystallization annealing temperature. The rapid

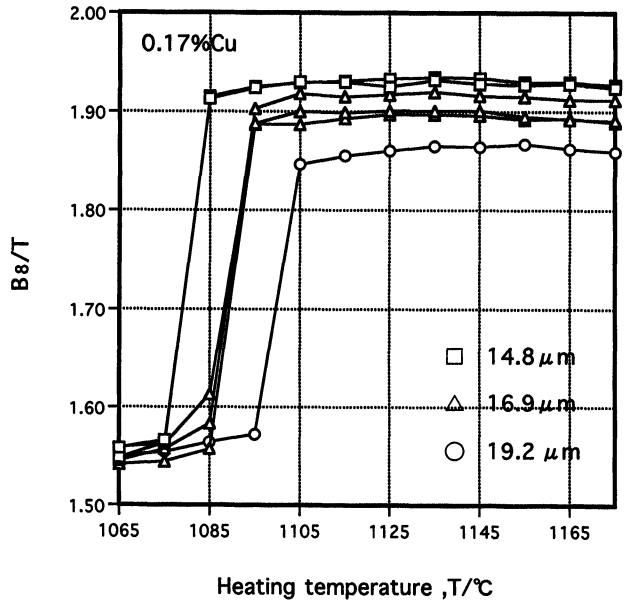

FIGURE 1 Relationship between magnetic induction B8 and heating temperature during secondary recrystallization annealing. 0.17%Cu.

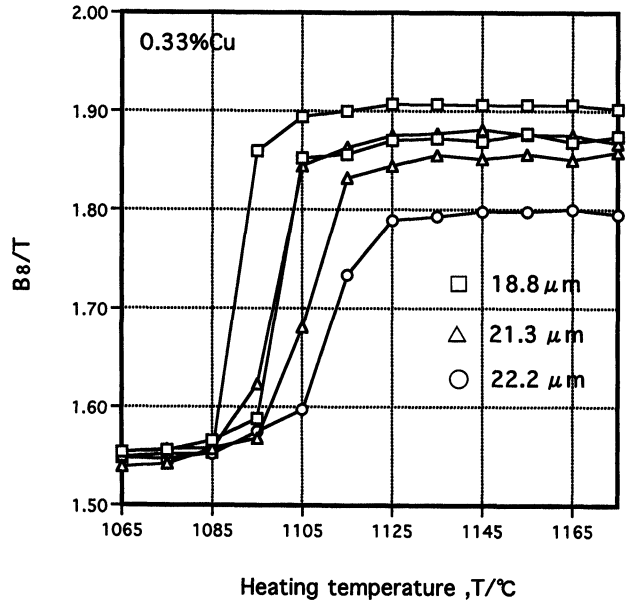

FIGURE 2 Relationship between magnetic induction B8 and heating temperature during secondary recrystallization annealing. 0.33%Cu.

increase in B8 corresponds to the onset of secondary recrystallization. Here regarding the temperature at B8 = 1.60 as the onset temperature of secondary recrystallization (T_{cr},) T_{cr} can be determined from these graphs.

The relationship between T_{cr} and the maximum B8 obtained from each graph (referred to as B8max) is shown in Fig. 3. It shows that increasing T_{cr} from 1075°C to 1100°C decreases B8max. It is shown elsewhere that B8max decreases again when T_{cr} is lower than about 1075°C when annealed in the same way as in this experiment (Harase *et al.*, 1995).

It has been reported in the case of SL that the highest B8 was obtained by the 1075°C-isothermal secondary recrystallization annealing with MgO coated on the specimen (Ushigami *et al.*, 1996c) in H_2–N_2 atmosphere, and B8 decreased either by decreasing or increasing in isothermal annealing temperature.

These results suggest that the evolution of a sharp Goss texture is to adjust the onset temperature of secondary recrystallization to be in the range of about 1075°C regardless of the annealing atmosphere either with or without MgO coating on the surface of the specimens.

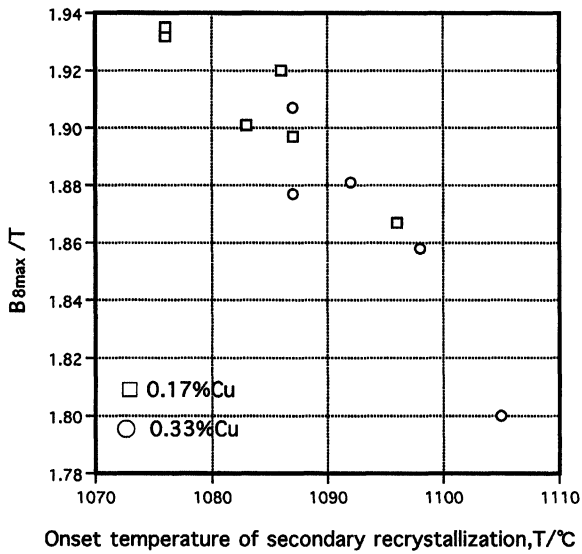

FIGURE 3 Relationship between the onset temperature of secondary recrystallization and B8max.

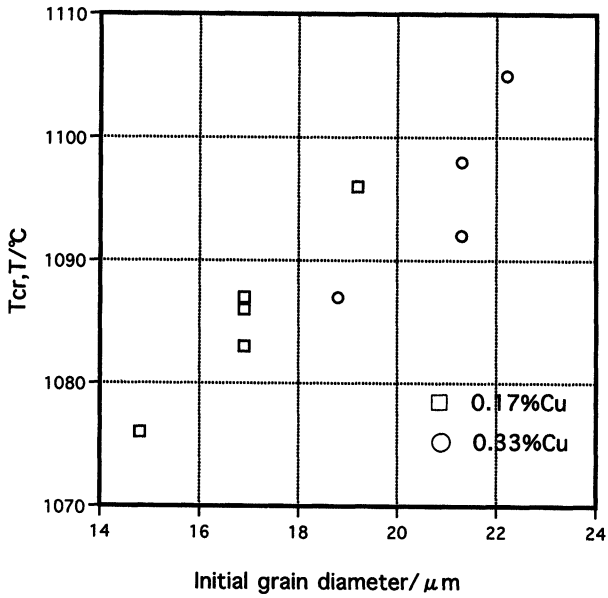

FIGURE 4 Influence of the initial grain diameter on the onset temperature of secondary recrystallization (T_{cr}).

Figure 4 shows the relationship between initial grain diameter and T_{cr}. It can be seen that T_{cr} increases with increasing initial grain diameter. This is the same tendency as that of the bicrystal experiment if T_{mj} in the bicrystal experiment corresponds to T_{cr}. in this experiment. Figure 5 shows the relationship between initial grain diameter and B8max. It can be seen that B8max decreases with increasing in initial grain diameter. This tendency is opposite to the tendency known in SL (Yoshitomi *et al.*, 1996). This suggests that the initial grain size itself does not directly determine the selective migration characteristics of the Σ9 boundary, but it affects T_{cr} and T_{cr} strongly influences the selective migration characteristics of the Σ9 boundary.

Figure 6 shows the relationship between initial nitrogen content and B8max. Data with the same grain size is connected in this graph. It shows that B8max increases with increasing initial nitrogen content, however, specimens with higher initial nitrogen content have relatively smaller grain diameters in this experiment, the influence of the initial grain diameter has to be taken into consideration. Figure 7 shows the relationship

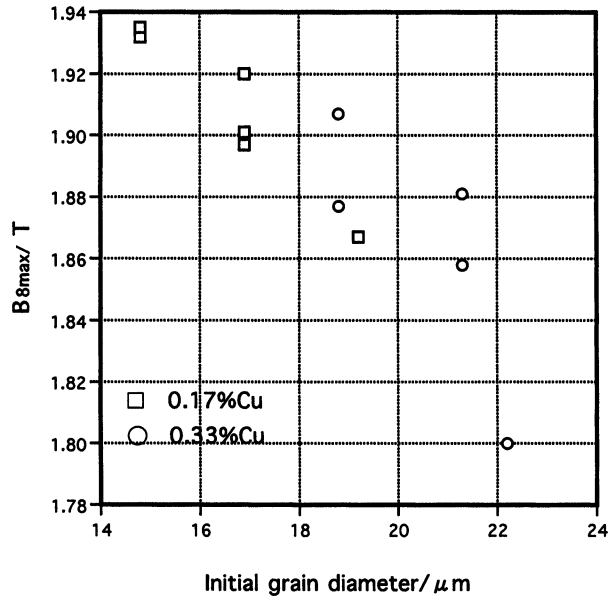

FIGURE 5 Relationship between the initial grain diameter and the maximum magnetic induction (B8max).

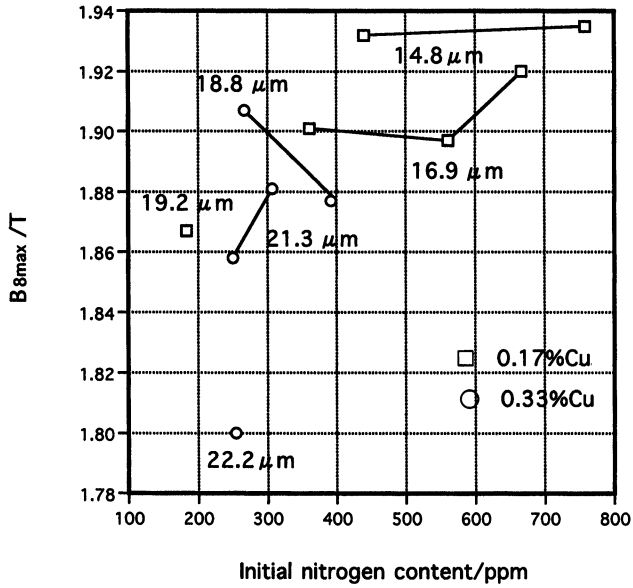

FIGURE 6 Relationship between the initial nitrogen content and the maximum magnetic induction (B8max).

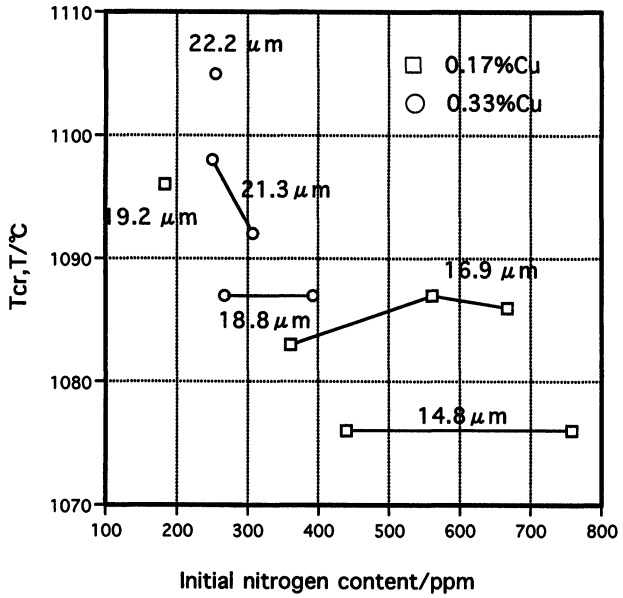

FIGURE 7 Influence of the initial nitrogen content on the onset temperature of secondary recrystallization (T_{cr}).

between initial nitrogen content and T_{cr}. Data with the same grain size is connected in this graph. It can be seen that the influence of the initial nitrogen content on T_{cr} is rather small and the influence of the initial grain size is large. It is concluded from this Model anneal that the evolution of the sharp Goss orientation is mainly determined by the onset temperature of secondary recrystallization and the initial grain size strongly affects the onset temperature of secondary recrystallization. The onset temperature for obtaining highest B8 value is around 1075°C and it is considered that Σ9 boundaries become most mobile at this temperature.

3.3.2. Box Anneal

The same primary specimens used for Model anneal (except for the specimen with 22.2 μm diameter) were annealed by Box anneal. Figure 8 shows the relationship between the initial grain diameter and B8 after secondary recrystallization annealing with MgO coating (Box anneal). It shows that increasing in initial grain size increases B8. This is the same

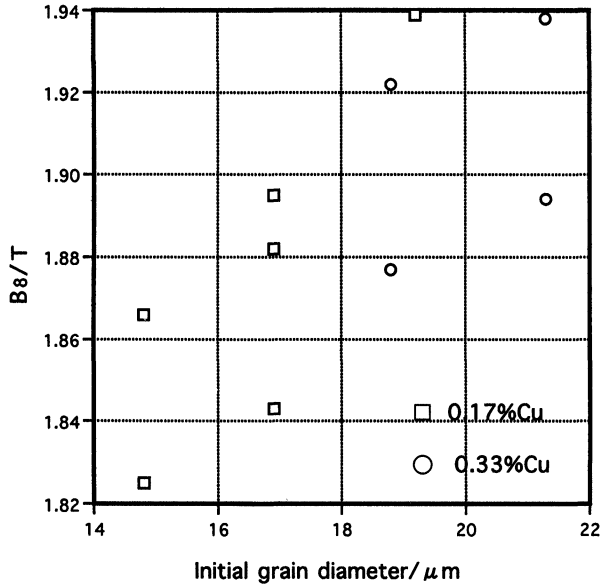

FIGURE 8 Influence of the initial grain diameter and the magnetic induction B8 after secondary recrystallization annealing with MgO coating.

tendency with SL, however, it is the opposite tendency to the Model anneal (see Fig. 5). Figure 9 shows the relationship between the initial nitrogen content and B8 by Box anneal. It shows that increasing in initial nitrogen content decreases B8. This is the opposite tendency to the Model anneal (see Fig. 6). As the specimens with higher nitrogen content have smaller initial grain diameter in this experiment, the influence of initial grain diameter has to be taken into consideration, however, the increasing in nitrogen content for the given grain size also decreases B8 in most cases. It is considered therefore that the increasing in initial nitrogen content tends to decrease B8 in the case of Box anneal.

In the Box anneal Mg_2SiO_4 is formed during secondary recrystallization annealing by the reaction of MgO and SiO_2 present on the surface layer of the specimen. It is reported that this Mg_2SiO_4 is somewhat impermeable to nitrogen and the nitrogen injected by nitriding treatment diffuses into the interior of the sheet and forms (Al, Si)N and very little nitrogen goes out from the specimen when the initial nitrogen content is about 200 ppm (Ushigami *et al.*, 1996a). It is also reported (Harase *et al.*, 1993) that the nitrogen content decreases to the constant

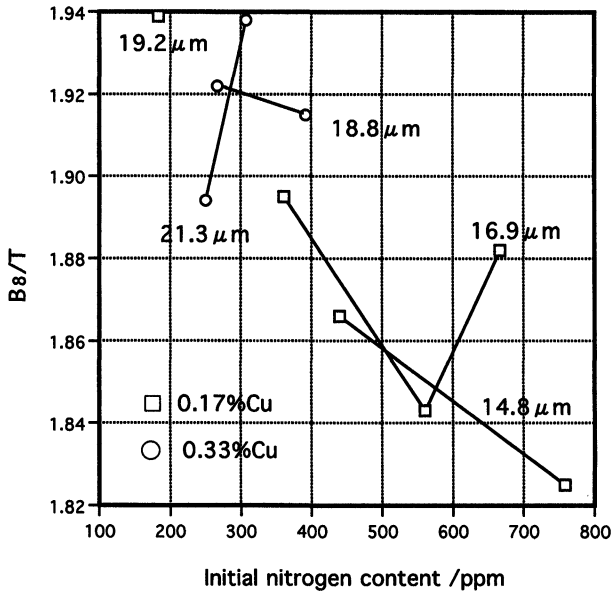

FIGURE 9 Influence of the initial nitrogen content on the magnetic induction B8 after secondary recrystallization annealing with MgO coating.

value of about 175 ppm in the temperature range between 975° and 1025°C during heating with 15°C/h in 25%H_2–N_2 in the specimen containing 0.026%Al and an initial nitrogen content between 200 and 280 ppm and coated with MgO. The nitrogen content during heating might change depending on the nature of Mg_2SiO_4 formed and the nitrogen partial pressure of the annealing atmosphere, the relative amount of nitrogen in the specimen with higher initial nitrogen content might be higher with MgO coating due to the impermeable nature of Mg_2SiO_4 compared with the specimen without Mg_2SiO_4. Contradictory results between Model anneal and Box anneal can be interpreted if we consider the impermeable nature of Mg_2SiO_4.

In the specimen with the smallest initial grain diameter of 14.8 μm containing 0.17%Cu, B8 was 1.87 T in the case of Box anneal when the initial nitrogen content was 440 ppm (see Fig. 9). The same specimen showed 1.93 T in the case of Model anneal (see Fig. 6) and T_{cr} was 1076°C (measured value, see Fig. 4). The inhibitor intensity of this specimen in the case of Box anneal might be higher due to the

impermeable nature of Mg_2SiO_4 and T_{cr} might be much higher than 1076°C resulting in the lower B8. It is therefore very probable that further decrease in B8 with increasing in initial nitrogen content from 440 to 793 ppm in the case of Box anneal (see Fig. 9) is attributed to the further increase in T_{cr}. Then it can be considered that B8 might increase by reducing the initial nitrogen content less than 440 ppm as T_{cr} will decrease to the optimum temperature of 1075°C with decreasing in nitrogen content. We will discuss this in the next section (see Fig. 10).

In the specimen with the largest initial grain diameter of 19.2 μm, in the specimen containing 0.17%Cu,the initial nitrogen content is as low as 183 ppm and it showed B8 = 1.94 T in the case of Box anneal (see Fig. 9). This suggests that T_{cr} of this specimen in the Box anneal will be around 1075°C. T_{cr} of this specimen in the Model anneal is 1096°C (measured) and B8max = 1.87 T (see Fig. 6). It is very likely that in the case of Box anneal no increase in nitrogen is expected due to the impermeable nature of Mg_2SiO_4, however, in the case of Model anneal increase in the nitrogen content is expected as the annealing atmosphere is 100%N_2 and no impermeable Mg_2SiO_4 is present resulting in the increase in T_{cr} as high as 1096°C. It is very probable in the Box anneal that increasing in nitrogen content higher than 183 ppm will then increase T_{cr} higher than 1075°C and decrease B8. We will discuss this in the next section (see Fig. 10).

It is thus possible to interpret the contradictory results obtained by Model anneal and Box anneal if we postulate that the highest B8 is obtained when the onset temperature of secondary recrystallization is around 1075°C and considering the nature of Mg_2SiO_4 formed in the case of Box anneal.

4. THE POSSIBILITY OF FURTHER IMPROVEMENT OF THE PRODUCTION TECHNOLOGY OF HI-B

It has become clear from the above discussion that the sharp Goss texture evolves when the onset temperature of secondary recrystallization is around 1075°C at which Σ9 boundaries become most mobile in the decarburized and nitrided Fe–3%Si alloy utilizing AlN as an inhibitor. Both HI-B and SL are subjected to high temperature hot band annealing followed by rapid cooling. If the metallurgical function of high

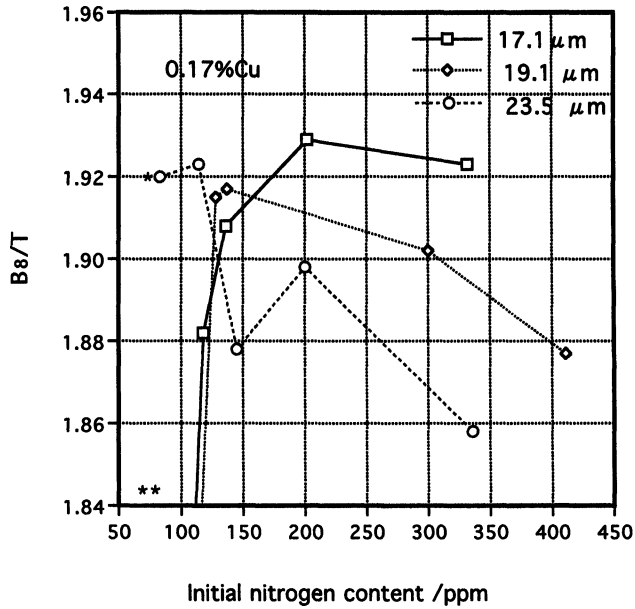

FIGURE 10 Influence of the initial nitrogen content on the magnetic induction B8 after secondary recrystallization annealing with MgO coating. The mark (*) denotes without nitriding treatment after decarburization annealing.

temperature annealing of hot band is to secure the fine precipitates of AlN by $\gamma \rightarrow \alpha$ transformation as an inhibitor, the necessity of high temperature annealing is not clear in the case of SL as AlN precipitates are mainly formed in the heating stage of secondary recrystallization annealing. The starting materials used in the present experiment would be almost α single phase in the high temperature range (the carbon content before cold rolling was 0.015%) and the hot band annealing temperature was as low as 900°C. A B8 value of about 1.94 was obtained when the onset temperature of secondary recrystallization is adjusted to be around 1075°C by selecting the initial grain diameter and nitrogen content according to the secondary recrystallization annealing method. To confirm the necessity of high temperature hot band annealing and the influence of the initial nitrogen content and grain diameter on B8 in the case of Box anneal, the hot rolled sheet with 0.17%Cu was annealed at 750°C × 30 min and quenched before cold rolling and processed in the

same way. In this experiment the initial nitrogen content is controlled to be less than about 400 ppm. The initial grain diameter was in the range between 17.1 and 23.5 μm. Figure 10 shows the influence of the initial nitrogen content and B8 after Box anneal. (*) in the graph denotes the data processed without nitriding after decarburization annealing. It shows that when the initial grain diameter is as large as 23.5 μm, 100% secondary recrystallization occurs even without nitriding after decarburization annealing (N = 80 ppm) and B8 decreases with increasing in nitrogen content. This indicates that the onset temperature of secondary recrystallization is about 1075°C when the initial nitrogen content is as low as 114 ppm and increases with increasing in nitrogen content resulting in the decrease in B8. When the initial grain diameter is as small as 17.1 μm, poor secondary recrystallization occurs without nitriding after decarburization annealing due to the larger driving force and weaker inhibitor intensity and B8 increased with increasing nitrogen content and became 1.93 T at the initial nitrogen content of 200 ppm and slightly decreased with increasing in the initial nitrogen up to 330 ppm.

This can be interpreted as T_{cr} at 200 ppm nitrogen is about 1075°C and it increases with increasing initial nitrogen content. When the initial grain diameter is 19.1 μm, poor secondary recrystallization occurred without nitriding after decarburization annealing and B8 increased when the nitrogen content is about 137 ppm and gradually decreased with increasing nitrogen content up to 411 ppm. It is very probable in this case that $T_{cr} = 1075$°C will be in the range of the initial nitrogen content between 137 and 300 ppm. This additional experiment clearly suggests that the precipitation of AlN by $\gamma \rightarrow \alpha$ transformation at the hot band annealing stage is not a prerequisite for the evolution of highly oriented Goss grains in this material. It shows the possibility of the production of HI-B without special nitriding after decarburization annealing or even hot band annealing itself.

As a subtle control of AlN precipitation is not necessary, and it is easy to determine the primary grain structure and the inhibitor intensity independently in the case of SL, the migration characteristics of coincidence boundaries and the mechanism of secondary recrystallization will be more deeply understood by utilizing SL and the possibility of the further development of the new technology of grain oriented silicon steel will increase.

5. CONCLUSIONS

(1) One stage cold rolling method (cold rolling reduction about 87%) is suitable for the production of grain oriented silicon steel with high permeability (HI-B) due to the distribution of Σ9 boundaries at the primary recrystallized stage. It is very difficult to produce HI-B with the two stage cold rolling method without controlling the distribution of nucleus orientation in the primary recrystallized stage.

(2) Primary recrystallized Fe–3%Si containing Al with grain diameters changing from 15 μm to 22 μm was nitrided. Nitrogen contents were in the range 183–793 ppm. They were then intermittently annealed with the heating rate of 15°C/h in 100%N_2 atmosphere. The maximum B8 obtained was about 1.94 T when the onset temperature of secondary recrystallization (T_{cr}) was around 1075°C regardless of the initial grain size or nitrogen content. The maximum B8 decreased with increasing T_{cr} from 1075°C to 1100°C. This result strongly suggested that Σ9 boundaries become most mobile around 1075°C regardless of the initial grain size or nitrogen content.

The same primary specimens were coated with MgO and annealed with the same heating rate in 5%H_2–N_2. The maximum B8 values obtained in this case were nearly the same as those obtained in the intermittent annealing, however, the initial grain size and nitrogen content for the maximum B8 was quite contrary in this annealing. The difference in the optimum grain size and nitrogen content for obtaining the highest B8 between both annealings was explained on the assumption that Σ9 boundaries become most mobile at 1075°C regardless of the annealing methods.

(3) It is demonstrated that the high temperature hot band annealing for the precipitation of AlN is not a prerequisite for the evolution of sharp Goss secondary recrystallization texture when the onset temperature of secondary recrystallization is controlled around 1075°C and the possibility of producing HI-B without hot band annealing and nitriding treatment after decarburization annealing.

References

Brandon, D.G. (1966). *Acta metall.*, **14**, 1479.
Goss, N.P. (1934). US Pat.1.965,559.

Goto, I., Matoba, I., Imanaka, T., Gotoh, T. and Kan, T. (1975). Development of a new grain-oriented silicon steel "RG-H" with high permeability. *Proc. Soft Mag. Mat.*, **2**, 262–268.

Harase, J., Shimizu, R., Kuroki, K., Nakayama, T., Wada, T. and Watanabe, T. (1985). Effect of primary recrystallization texture, orientation distribution and grain boundary characteristics on the secondary recrystallization behavior of grain-oriented silican steel having AlN and MnS as inhibitors. *Proc. 4th Inter. Symp. on Grain Boundary Structure and Related Phenomena*, Supplement of the Japan Institute of Metals, 563–570.

Harase, J., Shimizu, R., Takashima, K. and Watanabe, T. (1987). Effect of AlN on the secondary recrystallization of 3%Si–Fe Alloy. Transactions. *ISIJ.*, **27**, 965–973.

Harase, J. and Shimizu, R. (1990). Mechanism of secondary recrystallization in grain oriented silicon steel. *Journal of Japan Inst. Metals*, **54**, 1–8.

Harase, J., Shimizu, R., Yoshitomi, Y., Ushigami, Y. and Takahashi, N. (1993). Prediction of the texture evolved by grain growth. In *Inter. Symp. on Modeling of Coarsening and Grain Growth* Eds. by C.S. Pande and S.P. March. Fall Meeting of TMS in Chicago, 245–256.

Harase, J., Kurosawa, F., Ushigami, Y., Yoshitomi, Y. and Nakashimai, S. (1995). Change of magnetic induction of nitrided Fe–3%Si alloy during secondary recrystallization annealing. *J. of Japan Inst. Metals*, **59**, 917–924.

Nakayama, T., Ushigami, Y., Nagashima, T., Suga, Y. and Takahashi, N. (1996) Computer simulation of the influence of inhibitor intensity on secondary recrystallization in Fe–3%Si Alloy. *Materials Science Forum*, **204–206**, 611–616.

Ruer, D., Vadon, A. and Baro, B. (1979). *Text. Cryst. Solids*, **3**, 245.

Shimizu, R., Harase, J. and Dingley, D.J. (1990) Prediction of secondary recrystallization in Fe–3%Si by three dimensional texture analysis. *Acta metall*, **38**, 973–978.

Taguchi, S. and Sakakura, A. (1964). US Pat. 3,159,511.

Takahashi, N. and Harase, J. (1996). Recent development of technology of grain oriented silicon steel. *Materials Science Forum*, **204–206**, 143–154.

Takahashi, N., Suga, Y. and Kobayashi, H. (1996). Recent developments in grain-oriented silicon steel. *Journal of Magnetism and Magnetic Materials*, **160**, 98–101.

Tsurekawa, S., Ueda, T., Ichikawa, K., Nakashima, H., Yoshitomi, Y. and Yoshinaga, H. (1996). Grain boundary migration in Fe–3%Si bicrystal. *Materials Science Forum*, **204–206**, 221–226.

Ushigami, Y., Kurosawa, F., Masui, H., Suga, Y. and Takahashi, N. (1996a). Precipitation behaviors of injected nitride inhibitors during secondary recrystallization annealing in grain oriented silicon steel. *Materials Science Forum*, **204–206**, 593–598.

Ushigami, Y., Nakayama, T., Suga, Y. and Takahashi, N. (1996b). Influence of inhibitor intensity on secondary recrystallization in Fe–3%Si Alloy. *Materials Science Forum*, **204–206**, 599–604.

Ushigami, Y., Nakayama, T., Suga, Y. and Takahashi, N. (1996c). Influence of secondary recrystallization temperature on secondary recrystallization texture in Fe–3%Si Alloy. *Materials Science Forum*, **204–206**, 605–610.

Ushigami, Y., Yoshitomi, Y. and Takahashi, N. (1996d). Influence of primary recrystallized structure on secondary recrystallization in Fe–3%Si Alloy. *Materials Science Forum*, **204–206**, 623–628.

Yoshitomi, Y., Ushigami, Y., Takahashi, N., Nakayama, T., Suga, Y. and Harase, J. (1996). Prediction of sharpness of {110}⟨001⟩ secondary recrystallization texture of Fe–3%Si Alloy. *Materials Science Forum*, **204–206**, 629–634.